

Scaling of dynamical susceptibility at the onset of rigidity for disordered viscoelastic matter

Danilo B. Liarte,^{*} Stephen J. Thornton, Eric Schwen, Itai Cohen, Debanjan Chowdhury, and James P. Sethna
Department of Physics, Cornell University, Ithaca, NY 14853, USA

(Dated: December 24, 2024)

The onset of rigidity in interacting liquids, as they undergo a transition to a disordered solid, is associated with a dramatic rearrangement of the low-frequency vibrational spectrum. In this letter, we derive scaling forms for the singular dynamical response of disordered viscoelastic networks near both jamming and rigidity percolation. Using effective-medium theory, we extract critical exponents, invariant scaling combinations and analytical formulas for universal scaling functions near these transitions. Our scaling forms describe the behavior in space and time near the various onsets of rigidity, for rigid and floppy phases and the crossover region, including diverging length and time scales at the transitions. We expect that these behaviors can be measured in systems ranging from colloidal suspensions to anomalous charge-density fluctuations of “strange” metals.

Disordered viscoelastic materials exhibit fascinating invariant scaling behavior associated with deformation and the onset of rigidity [1]: from depinning [2] and plastic yielding [3] to rigidity percolation (RP) [4] and jamming [5]. The latter two are often described by elastic network models near the Maxwell limit of mechanical stability [6], and represent transitions from a rigid phase to a floppy one when the average coordination number z falls below the isostatic value z_c . But whereas jamming is commonly described in terms of sphere packings that resist compression and thus possess a finite bulk modulus $B > 0$ at the transition, RP is described in terms of networks in which bonds are randomly removed and that do not resist compression ($B = 0$) [7] at the transition [8–10]. Despite the ubiquity of the jamming transition [5, 11], the scarcity of analytical models (except for high-dimensional sphere packings [12–14]) and comprehensive numerical data describing its universal properties have delayed the development of unifying scaling theories such as Ref. [15]. Here we leverage the analytically-tractable effective-medium theory (EMT) of Ref. [16] to compute general universal scaling forms for susceptibilities and space-time correlations near jamming and RP.

At jamming [5], two-dimensional disk packings form a disordered contact network [blue lines in Fig. 1(a)] that supports compression but not shear. Mimicking compression by randomly adding next-nearest neighbor bonds between disks [red N-bonds in Fig. 1(a)] and/or randomly removing B-bonds can lead to either jamming or RP depending on the population for each type of bond [16]. A simpler model that yields the same scaling behavior consists of randomly placing ‘B’ and ‘N’-bonds between nearest and next-nearest neighbor pairs of sites [blue and red solid lines in Fig. 1(b)] of a periodic honeycomb lattice. This network describes a diluted version of a 3-sublattice system consisting of a honeycomb lattice [shaded blue in Fig. 1(b)] and two triangular lattices (shaded red; here we show only the bonds of one triangular lattice). Detailed knowledge of the mechanical behavior of periodic lattices allowed the development of an EMT for jam-

ming [16] valid in both the rigid and floppy states, and for the crossover from jamming to RP. We will employ these results to derive *explicit solutions* for the critical scaling of the susceptibilities of disordered viscoelastic matter near jamming and RP. Our explicit analysis not only allows for quick assessment of scale-invariant behavior of quantities such as viscosities and correlations (without the need for computationally-expensive simulations); it also serves as an example of how one may analyze rigidity transitions for which the universality class has not yet been determined.

Figure 1(c) shows the phase diagram of the honeycomb-triangular lattice (HTL) model in terms of occupation probability of nearest neighbor B bonds and next-nearest neighbor N bonds. Rigid (yellow) and floppy regions are separated by an RP line that terminates in a multicritical jamming point J (red disk). Arrows denote paths approaching jamming and RP from the rigid and floppy states. From Fig. 1(c), one can also extract definitions for the scaling variables δp_B and δp_{RP} , chosen so that $\delta p_{RP} = 0$ at RP, and δp_B is also zero at jamming.

RP should generically be codimension one, because only one constraint (isostaticity) needs to be satisfied. In the HTL model of Fig. 1(b), jamming is codimension two. But the jump in bulk modulus characteristic of jamming here demands a complete honeycomb lattice; one can see that if the three orientations of hexagon bonds were independently populated, the jamming transition would be codimension four (their three probabilities set to one plus isostaticity). This special tuning of the system to favor the bulk modulus is echoed in the jamming of frictionless spheres, where the first state of self stress [17] leads to a jump in the bulk modulus because the conjugate degree of freedom (a uniform compression) was used to tune the system to the rigidity transition. As evidence for this, shear jamming of frictionless spheres has a jump in a single anisotropic modulus [18].

We conjecture that there is a class of disordered elastic systems for which a renormalization-group scheme leads

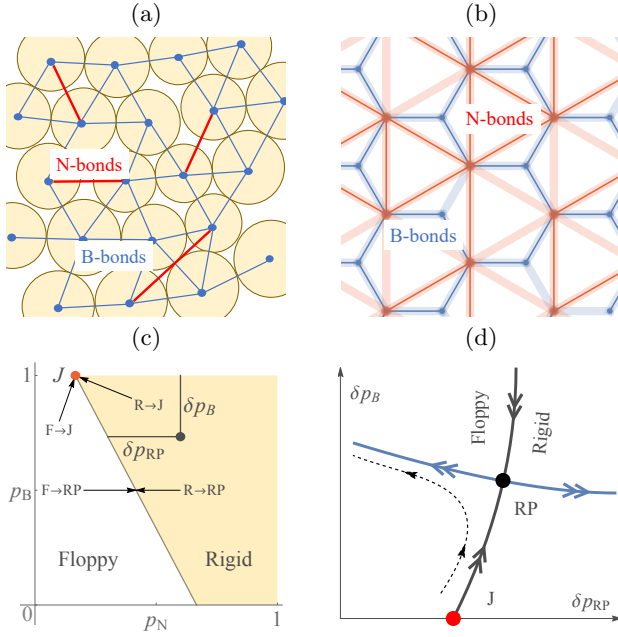


FIG. 1. (a) Jammed disk packing, underlying contact network (B-bonds in blue) and randomly added next-nearest neighbor N-bonds (red). (b) HTL model with nearest and next-nearest neighbor bonds (solid blue and red lines) connecting sites of a honeycomb lattice. Faint blue and red lines show underlying honeycomb and triangular lattices, respectively. (c) Phase diagram of the HTL model in terms of occupation probabilities for B and N-bonds. The yellow region corresponds to the rigid state, and is separated from the floppy state by an RP line ending at a jamming point J (red disk). The arrows show paths approaching jamming and RP from both phases. (d) Conjecture for a crossover flow diagram projected into $\delta p_{RP} \times \delta p_B$ space. J (red disk) and RP (black disk) represent fixed points of a putative renormalization-group scheme. The blue and black solid lines and the black dashed line represent the unstable manifold, the critical line and a sample trajectory, respectively.

to the typical crossover flow diagram [19] (projected in $\delta p_{RP} \times \delta p_B$ space) illustrated in Fig. 1(d). The scaling variable $\delta p_{RP} \propto \Delta z \equiv z - z_c$ must be relevant for both jamming and RP, but the depletion probability of the B-lattice δp_B is relevant only for jamming. This behavior is captured by the direction of the arrows coming in and out of the putative jamming and RP fixed points (red and black disks, respectively) in Fig. 1(d). A system near the J fixed point ($\delta p_B, |\delta p_{RP}| \ll 1$) will be controlled either by J if a crossover variable $\delta p_B/|\delta p_{RP}|^\varphi \ll 1$ for some exponent φ , or by RP if $\delta p_B/|\delta p_{RP}|^\varphi \gg 1$, i.e. for trajectories such as the black dashed line passing sufficiently close to the critical line (black solid line.) Though δp_B does not have a direct interpretation in the jamming of sphere packings [except for the network model of Fig. 1(a)], there might be variables that play a similar role, such as attractive interactions in soft gels [20].

We now introduce a scaling *ansatz* for the longitudinal

response function [21] near jamming:

$$\chi_L \approx |\delta p_{RP}|^{-\gamma} \mathcal{L} \left(\frac{q}{|\delta p_{RP}|^\nu}, \frac{\omega}{|\delta p_{RP}|^{z\nu}}, \frac{\delta p_B}{|\delta p_{RP}|^\varphi} \right), \quad (1)$$

where q is the wavevector, ω is the frequency, γ , ν , z and φ are critical exponents for the susceptibility, correlation length, correlation time, and crossover behavior, respectively [19, 22], and \mathcal{L} is a universal scaling function. Many other properties can be derived from \mathcal{L} (Table II). Such space-time susceptibilities, and the corresponding structure and correlation functions, are the fundamental linear response quantities for materials. They have been well studied in glassy systems, but have hitherto not been a focus in the study of jamming or RP. Baumgarten et al. [23] and Hexner et al. [24] have studied the static response of frictionless jammed spheres to a sinusoidal perturbation; they find diverging length scales that are different from the ones presented here. Because our system is on a regular lattice, and particularly because our analysis replaces the disordered lattice with a uniform one, it is natural for us to fill this gap.

Our approach goes beyond previous work [15] in two aspects. First, rather than starting with an ansatz for the free energy in terms of the excess contact number Δz , excess packing fraction $\Delta\phi$, shear stress ϵ and system size N , we consider the longitudinal response in terms of δp_{RP} , q , ω and δp_B . Our variable δp_{RP} is proportional to Δz . Though we do not consider an explicit dependence of χ_L on ϵ or $\Delta\phi$ [25], we can extract equivalent expressions for moduli and correlations from the dependence of χ_L on q . Importantly, the inclusion of ω in our analysis allows us to predict dynamical properties such as viscosities.

Second, we use EMT [16] to derive and validate both the universal exponents and the universal scaling functions (\mathcal{L}), for both jamming and RP. This form of EMT is based on the coherent-potential approximation [8, 26] (CPA), and is known to reproduce well results obtained from simulations of randomly-diluted lattices with two-body [27] harmonic interactions [28, 29], even for undamped [9, 16] and overdamped dynamics [30, 31]. Although the CPA involves mean-field-like uncontrolled approximations, it preserves the topology of the original lattices — an essential ingredient that ultimately allows one to describe jamming. Here we focus on the longitudinal response, since the full response of isotropic elastic systems can be decomposed into longitudinal and transverse components, and the latter has the same scaling form near both jamming and RP as the longitudinal response near RP; see Supplemental Material (SM) [32].

We use the long wavelength limit of the longitudinal response χ_L along with EMT results from Ref. [16] to derive critical exponents (see Table I) and the universal scaling function \mathcal{L} in Eq. (1) (see SM [32]),

$$\mathcal{L}(u, v, w) = \left[\frac{a u^2}{1 + w/\mathcal{M}_\pm(v)} - \tilde{v}(v) \right]^{-1}. \quad (2)$$

Here $\mathcal{M}_{\pm}(v) = b \left[\sqrt{1 - c\tilde{v}(v)} \pm 1 \right]$ and a , b and c are constants. The plus and minus signs in \mathcal{M}_{\pm} correspond to solutions in the elastic and floppy states, respectively. Finally, $\tilde{v}(v) = \rho v^2$ and $i\gamma v$ for undamped and overdamped dynamics, respectively, where ρ is a mass density and γ is a drag coefficient. Equation (2) embodies the central results of this paper. From Eqs. (1) and (2), we will extract the universal behavior of the elastic moduli, viscosities as well as the density response and correlation functions (dynamic structure factor). Though it is not certain that these functions are as universal as critical exponents, recent simulations of compressed hyperspheres [33] indicate that critical amplitudes calculated using mean-field models at infinite dimension are preserved for low-dimensional jammed packings.

	γ	z	ν	φ	β_B	γ_B
Jamming	2	1 (2)	1	1	0	1 (2)
Rigidity Percolation	2	2 (4)	1/2	-	1	0 (1)

TABLE I. Critical exponents for the longitudinal susceptibility (γ), correlation length (ν), correlation time (z) and crossover behavior (φ) near jamming and RP for undamped and overdamped (between parentheses if different from undamped) dynamics. The exponents β_B and γ_B can be derived from γ , ν and z (see Table II), and describe power-law singularities for the bulk modulus and viscosity, respectively.

For $|\delta p_{RP}| \ll \delta p_B$ [$w \gg 1$ in Eq. (2)], our model exhibits RP criticality: δp_B becomes an irrelevant variable, and $\mathcal{L}(u, v, w) \rightarrow \tilde{\mathcal{L}}(u, v)$, with

$$\tilde{\mathcal{L}}(u, v) = [a' u^2 \mathcal{M}_{\pm}(v) - \tilde{v}(v)]^{-1}. \quad (3)$$

Here $a' = a/\delta p_B$ is a constant, and the change in \mathcal{L} is accompanied by a change in the critical exponents ν and z (see Table I). Note that the invariant scaling combinations $q/|\delta p_{RP}|^{\nu}$ and $\omega/|\delta p_{RP}|^{z\nu}$ lead to definitions for diverging length and time scales, $\ell^* \sim 1/|\delta p_{RP}|^{\nu}$ and $\tau^* \sim 1/|\delta p_{RP}|^{z\nu}$, respectively. The exponent $z\nu$ depends only on the type of dynamics, but the exponent ν (equals 1 and 1/2 for jamming and RP, respectively) emerges naturally in our approach and is consistent with more elaborate definitions involving cutting boundaries [11].

To validate Eqs. (2) and (3), we show in Fig. 2 the scaling collapse plots of the longitudinal response as a function of the frequency scaling combination $v = \omega/|\delta p_{RP}|^{z\nu}$, near jamming and RP, for overdamped dynamics, in the rigid and floppy phases. The solid and dashed curves are the asymptotic universal scaling predictions at two different values of the wavevector scaling variable $u = q/|\delta p_{RP}|^{\nu}$. We approach the jamming point along paths of constant $\delta p_B/|\delta p_{RP}|^{\varphi} \equiv w$. Real parts are in blue; imaginary (dissipative) parts in red. Symbols show the convergence of the full solutions of the EMT equations to our universal scaling forms (Eqs. (2) and (3)).

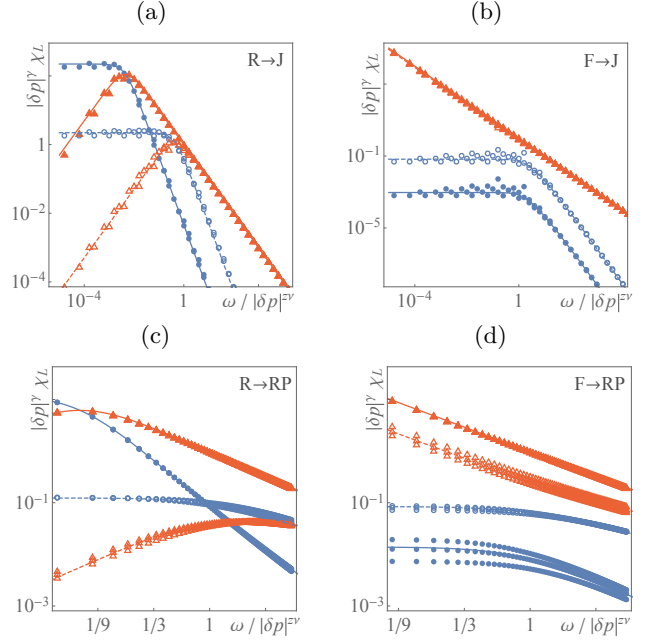


FIG. 2. Scaling collapse of the longitudinal response near jamming and RP for overdamped dynamics following the paths shown in Fig. 1(c). Blue disks and red triangles correspond to full solutions of the EMT equations for the real and imaginary parts of $|\delta p_{RP}|^{\gamma} \chi_L$, respectively. Solid and dashed curves correspond to the universal scaling predictions of Eqs. (2) and (3). Dashed [solid] lines correspond to $q/|\delta p_{RP}|^{\nu} = u = 1$ [0.1]. We approach the jamming point along $\delta p_B/|\delta p_{RP}|^{\varphi} \equiv w$ equal to $\sqrt{5}/4$ from the rigid side (a), and equal to 2 from the floppy side (b). Simulations run at $|\delta p_{RP}| = 10^{-2}$, 10^{-3} , and 10^{-4} for RP and a range $|\delta p_{RP}| \in [5 \times 10^{-2}, 5 \times 10^{-6}]$ for jamming show convergence to our universal asymptotic predictions.

The universal function \mathcal{L} (and $\tilde{\mathcal{L}}$) describes the scale-invariant behavior of the longitudinal response. On the overdamped solid side [Fig. 2(a) and (c)], the real part $\mathcal{L}'(v)$ plateaus and the imaginary part $\mathcal{L}''(v)$ (the dissipation) vanishes at low frequency v . At high frequency, both \mathcal{L}' and \mathcal{L}'' decay to zero, but \mathcal{L}' decays faster than \mathcal{L}'' [34]. This leads to a frequency scale above which $\mathcal{L}'' > \mathcal{L}'$ in the “diffusive limit” $\omega/q^2 \sim D^*$, where $D^* \sim |\delta p_{RP}|^{\psi}$ is a characteristic diffusion constant, with the exponent $\psi \equiv (z-2)\nu$ equal to zero and one for jamming and RP, respectively. The precise form of the decay of \mathcal{L}' and \mathcal{L}'' depends on the wavevector u (see SM [32]). On the liquid side, \mathcal{L}' behaves as in the solid side, but \mathcal{L}'' diverges rather than vanishing at low v due to the predominant viscous response of the liquid state.

Equations (1) and (2) determine the scaling behavior of several quantities characterized by the general form,

$$Y = |\delta p_{RP}|^y \mathcal{Y} \left(\frac{q}{|\delta p_{RP}|^{\nu}}, \frac{\omega}{|\delta p_{RP}|^{z\nu}}, \frac{\delta p_B}{|\delta p_{RP}|^{\varphi}} \right), \quad (4)$$

where in Table II we present explicit expressions for the

exponent y and universal function \mathcal{Y} describing the bulk modulus (B), viscosity (ζ), density response (Π) and correlation function (S). The behavior near RP is obtained by replacing \mathcal{Y} and \mathcal{L} in the third column of Table II by $\bar{\mathcal{Y}}$ and $\bar{\mathcal{L}}$ (now functions of u and v only), respectively, along with appropriate changes for the exponents (see Table I). The scaling behavior of the shear modulus and viscosity near jamming and RP is the same as that of B and ζ , respectively, near RP.

Y	y	\mathcal{Y}
B	$\beta_B \equiv \gamma - 2\nu$	$\mathcal{B} = (\partial \mathcal{L}^{-1} / \partial u) / (2u)$
ζ	$-\gamma_B \equiv \gamma - (2+z)\nu$	$\mathcal{Z} = (1/v) \text{Im}[\mathcal{B}]$
Π	$2\nu - \gamma$	$\mathcal{P} = d' u^2 \mathcal{L}$
S	$(2+z)\nu - \gamma$	$\mathcal{S} = (2T/v) \text{Im}[\mathcal{P}]$

TABLE II. Critical exponent y and universal scaling function \mathcal{Y} describing the singular behavior of the bulk modulus B and viscosity ζ , density response Π and correlation function S , according to Eq. (4).

We now discuss an intriguing application of our universal function $\bar{\mathcal{S}}(u, v)$ (see Table II) for the density-density correlation (the structure function for isotropic fluids at $q \neq 0$), shown in Fig. 3(a) for undamped fluids near RP. At fixed u , $\bar{\mathcal{S}}(u, v)$ has a maximum (blue dashed line) at $v = v^* \approx \mathcal{O}(1)$ [i.e. $\omega^* \propto \delta p_{\text{RP}}$] (see SM [32]), which coincides with the crossover from Debye to iso-static behavior, interpreted as the paradigmatic *boson peak* [35, 36] of glasses [37]. Near jamming or RP, this point marks the onset of the enhancement of the population of low-energy modes [38] leading to a flat density of states at low frequency [16, 38]. We will analyze the surprising connections between these featureless low-energy modes and the unconventional *particle-hole continuum* measured recently using momentum and energy-resolved spectroscopic probes in certain *strange metals* [39, 40] in Ref. [41]. The damping of the *plasmon* into the broad, featureless continuum in the cuprate strange metal [39] is possibly related to the behavior of the longitudinal response analyzed in this paper; we leave a detailed discussion of this analogy for elsewhere [41]. At fixed v , $\bar{\mathcal{S}}$ plateaus at a value of u of $\mathcal{O}(1)$ (i.e. at $q \propto |\delta p_{\text{RP}}|^{1/2}$). Figure 3(b) shows a diagram in terms of u and v marking the boson peak (blue-dashed line) and regions where $\bar{\mathcal{S}}(u, v)$ exhibits power-law behavior. The blue region indicates the neighborhood of the boson peak, in which $\bar{\mathcal{S}}(u, v) > \bar{\mathcal{S}}(u, v^*)/2$, and the red and yellow regions show power-law regimes in the rescaled frequency v and wavevector u .

In this letter, we have combined scaling theory and the EMT of Ref. [16] to produce analytical formulas for universal scaling functions for the longitudinal dynamical response near both jamming and RP. Our equations can be used to determine the space-time dependence of

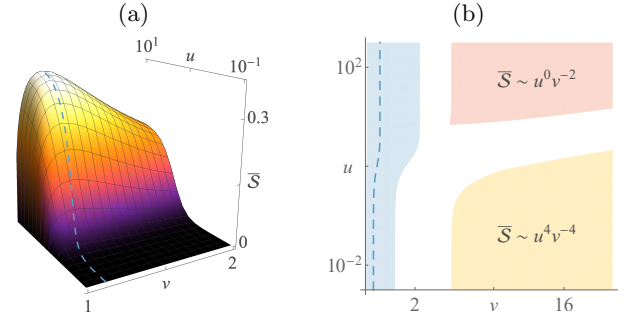


FIG. 3. (a) 3D plot of the universal scaling function for the correlation function $\bar{\mathcal{S}}(u, v)$, for undamped fluids near RP. The blue dashed line corresponds to the rescaled frequency v^* (the boson peak) at which $\bar{\mathcal{S}}(u, v)$ is maximum for fixed rescaled wavevector u . (b) $u \times v$ diagram showing the boson peak (blue dashed line) and power law regions for which $\bar{\mathcal{S}}(u, v) \propto u^\alpha v^\beta$, with (α, β) within 10% of their asymptotic values $(0, -2)$ (red) and $(4, -4)$ (yellow). In the blue region the condition $\bar{\mathcal{S}}(u, v) > \bar{\mathcal{S}}(u, v^*)/2$ is satisfied.

universal functions for several quantities (as moduli, viscosities and correlations) near the onset of rigidity in both the solid and liquid phases. A direct approach to experimentally validate our predictions consists in using 3D printers to fabricate and perform experiments on the disordered elastic networks illustrated in Figs. 1(a) and (b). We also expect these scaling forms to apply to more traditional glass forming systems such as colloidal suspensions. Here, in addition to more standard scattering measurements, new techniques for measuring 3D particle positions and even stresses with high precision may make it feasible to measure these functional forms and test our predictions [42–45].

In such suspensions, we expect that the scaling functions will capture the behavior in the elastic regime. However, our theory is built on a fixed network topology and lacks some features of the liquid phase. Annealed rather than quenched disorder [19] (or even intermediate disorder [46]) could be needed to describe viscoelastic fluids. Extensions of our analysis could include the incorporation of *anisotropic* bond occupation [47], which can lead to simpler models for both shear jamming [48] and thickening [49], and random stress fields, which can elucidate the unjamming of colloidal suspensions (such as titanium dioxide) due to activity [50].

We thank Andrea Liu, Daniel Hexner, Emanuela del Gado, Matthieu Wyart, Meera Ramaswamy, Peter Abbatonte, Sean Ridout, Tom Lubensky and Xiaoming Mao for useful conversations. This work was supported in part by NSF DMR-1719490 (ST and JPS), NSF CBET Award # 2010118 (DBL, ES, JPS, and IC) and NSF CBET Award # 1509308 (ES and IC). DC is supported by a faculty startup grant at Cornell University.

* liarte@cornell.edu

- [1] J. P. Sethna, M. K. Bierbaum, K. A. Dahmen, C. P. Goodrich, J. R. Greer, L. X. Hayden, J. P. Kent-Dobias, E. D. Lee, D. B. Liarte, X. Ni, K. N. Quinn, A. Raju, D. Z. Rocklin, A. Shekhawat, and S. Zapperi, *Annual Review of Materials Research* **47**, 217 (2017).
- [2] D. S. Fisher, *Physics Reports* **301**, 113 (1998).
- [3] F. F. Csikor, C. Motz, D. Weygand, M. Zaiser, and S. Zapperi, *Science* **318**, 251 (2007).
- [4] M. Thorpe, *Journal of Non-Crystalline Solids* **57**, 355 (1983).
- [5] A. J. Liu and S. R. Nagel, *Annual Review of Condensed Matter Physics* **1**, 347 (2010), <https://doi.org/10.1146/annurev-conmatphys-070909-104045>.
- [6] J. C. M. F.R.S., *The London, Edinburgh, and Dublin Philosophical Magazine and Journal of Science* **27**, 294 (1864), <https://doi.org/10.1080/14786446408643668>.
- [7] Different types of lattices do not *appear* to have the same universal RP behavior. For instance, isotropic periodic Maxwell lattices (in which $z = z_c = 2D$ where D is the dimension) can have $B, G > 0$ (as in the kagome lattice), where G is the shear modulus, or $B = 0$ and $G > 0$ (as in the twisted-kagome lattice, see e.g. [29]), which suggests that these lattices do not belong to the same RP universality class. However, if these lattices have extra bonds so that $z > 2D$, arbitrary protocols to randomly dilute these networks without specifically targeting particular bonds will lead to a continuous transition for both B and G .
- [8] S. Feng, M. F. Thorpe, and E. Garboczi, *Physical Review B* **31**, 276 (1985).
- [9] X. Mao and T. C. Lubensky, *Phys. Rev. E* **83**, 011111 (2011).
- [10] D. B. Liarte, O. Stenull, X. M. Mao, and T. C. Lubensky, *Journal of Physics-Condensed Matter* **28**, 165402 (2016).
- [11] A. J. Liu, S. R. Nagel, W. Van Saarloos, and M. Wyart, *Dynamical heterogeneities in glasses, colloids, and granular media*, 298 (2011).
- [12] J. Kurchan, G. Parisi, and F. Zamponi, *Journal of Statistical Mechanics: Theory and Experiment* **2012**, P10012 (2012).
- [13] J. Kurchan, G. Parisi, P. Urbani, and F. Zamponi, *The Journal of Physical Chemistry B* **117**, 12979 (2013), PMID: 23581562, <https://doi.org/10.1021/jp402235d>.
- [14] P. Charbonneau, J. Kurchan, G. Parisi, P. Urbani, and F. Zamponi, *Journal of Statistical Mechanics: Theory and Experiment* **2014**, P10009 (2014).
- [15] C. P. Goodrich, A. J. Liu, and J. P. Sethna, *Proceedings of the National Academy of Sciences* **113**, 9745 (2016), <https://www.pnas.org/content/113/35/9745.full.pdf>.
- [16] D. B. Liarte, X. Mao, O. Stenull, and T. C. Lubensky, *Phys. Rev. Lett.* **122**, 128006 (2019).
- [17] T. C. Lubensky, C. L. Kane, X. Mao, A. Souslov, and K. Sun, *Reports on Progress in Physics* **78**, 073901 (2015).
- [18] M. Baity-Jesi, C. P. Goodrich, A. J. Liu, S. R. Nagel, and J. P. Sethna, *Journal of Statistical Physics* **167**, 735 (2017).
- [19] J. Cardy, *Scaling and renormalization in statistical physics* (Cambridge university press, 1996).
- [20] E. del Gado and X. Mao, personal communication (2020).
- [21] P. Chaikin and T. Lubensky, *Principles of Condensed Matter Physics* (Cambridge University Press, Cambridge, 1995).
- [22] J. Sethna, *Statistical mechanics: entropy, order parameters, and complexity* (Oxford University Press, 2006).
- [23] K. Baumgarten, D. Vågberg, and B. P. Tighe, *Phys. Rev. Lett.* **118**, 098001 (2017).
- [24] D. Hexner, S. R. Nagel, and A. J. Liu, “The length dependent elasticity for jammed systems,” Poster presented at CECAM workshop, *Recent Advances on the Glass and Jamming Transitions*, (2017).
- [25] Note that δp_{RP} does not change with lattice deformation for our system. This contrasts with the case of compressed disks in which Δz can vary with $\Delta \phi$. We assume fixed (quenched) disorder in our model.
- [26] R. J. Elliott, J. A. Krumhansl, and P. L. Leath, *Rev. Mod. Phys.* **46**, 465 (1974).
- [27] A more sophisticated version of EMT is needed to reproduce the scaling behavior of randomly-diluted lattices with three-body forces such as bending [10].
- [28] L. M. Schwartz, S. Feng, M. F. Thorpe, and P. N. Sen, *Phys. Rev. B* **32**, 4607 (1985).
- [29] D. B. Liarte, O. Stenull, and T. C. Lubensky, *Phys. Rev. E* **101**, 063001 (2020).
- [30] M. G. Yucht, M. Sheinman, and C. P. Broedersz, *Soft Matter* **9**, 7000 (2013).
- [31] G. Duering, E. Lerner, and M. Wyart, *Soft Matter* **9**, 146 (2013).
- [32] See Supplemental Material at [URL will be inserted by publisher] for a brief review of the main results of Ref. [16], details for the derivation of the critical exponents and universal scaling functions for the longitudinal response, as well as scaling collapse plots near both jamming and rigidity percolation for undamped and overdamped dynamics in the rigid and floppy phases, and derivations for the universal scaling behavior of the transverse dynamic response, bulk modulus and viscosity, density response and correlation functions.
- [33] J. D. Sartor, S. A. Ridout, and E. I. Corwin, *Phys. Rev. Lett.* **126**, 048001 (2021).
- [34] This is true except in the limit of very large u and v , where both \mathcal{L}' and \mathcal{L}'' decay as $v^{-1/2}$. See SM [32] for details.
- [35] V. Vitelli, N. Xu, M. Wyart, A. J. Liu, and S. R. Nagel, *Phys. Rev. E* **81**, 021301 (2010).
- [36] E. DeGiuli, A. Laversanne-Finot, G. Düring, E. Lerner, and M. Wyart, *Soft Matter* **10**, 5628 (2014).
- [37] K. Binder and W. Kob, *Glassy materials and disordered solids: An introduction to their statistical mechanics* (World scientific, 2011).
- [38] L. E. Silbert, A. J. Liu, and S. R. Nagel, *Phys. Rev. Lett.* **95**, 098301 (2005).
- [39] M. Mitrano, A. A. Husain, S. Vig, A. Kogar, M. S. Rak, S. I. Rubeck, J. Schmalian, B. Uchoa, J. Schneeloch, R. Zhong, G. D. Gu, and P. Abbamonte, *Proceedings of the National Academy of Sciences* **115**, 5392 (2018), <https://www.pnas.org/content/115/21/5392.full.pdf>.
- [40] A. A. Husain, M. Mitrano, M. S. Rak, S. Rubeck, B. Uchoa, K. March, C. Dwyer, J. Schneeloch, R. Zhong, G. D. Gu, and P. Abbamonte, *Phys. Rev. X* **9**, 041062 (2019).
- [41] S. J. Thornton, D. B. Liarte, J. P. Sethna, and

- D. Chowdhury, “Jamming and unusual charge density fluctuations of strange metals,” (2021), in preparation.
- [42] E. R. Weeks, J. C. Crocker, A. C. Levitt, A. Schofield, and D. A. Weitz, *Science* **287**, 627 (2000).
 - [43] N. Y. Lin, M. Bierbaum, P. Schall, J. P. Sethna, and I. Cohen, *Nature materials* **15**, 1172 (2016).
 - [44] M. Bierbaum, B. D. Leahy, A. A. Alemi, I. Cohen, and J. P. Sethna, *Phys. Rev. X* **7**, 041007 (2017).
 - [45] B. D. Leahy, N. Y. Lin, and I. Cohen, *Current Opinion in Colloid & Interface Science* **34**, 32 (2018).
 - [46] E. do Carmo, D. B. Liarte, and S. R. Salinas, *Phys. Rev. E* **81**, 062701 (2010).
 - [47] T. Zhang, J. M. Schwarz, and M. Das, *Phys. Rev. E* **90**, 062139 (2014).
 - [48] R. P. Behringer and B. Chakraborty, *Reports on Progress in Physics* **82**, 012601 (2018).
 - [49] E. Brown and H. M. Jaeger, *Reports on Progress in Physics* **77**, 046602 (2014).
 - [50] S. Henkes, Y. Fily, and M. C. Marchetti, *Phys. Rev. E* **84**, 040301 (2011).